# AROME-MetCoOp: A Nordic Convective-Scale Operational Weather Prediction Model

MALTE MÜLLER,[a] MARIKEN HOMLEID,[a] KARL-IVAR IVARSSON,[b] MORTEN A. Ø. KØLTZOW,[a] MAGNUS LINDSKOG,[b] KNUT HELGE MIDTBØ,[a] ULF ANDRAE,[b] TRYGVE ASPELIEN,[a] LARS BERGGREN,[b] DAG BJØRGE,[a] PER DAHLGREN,[c] JØRN KRISTIANSEN,[a] ROGER RANDRIAMAMPIANINA,[a] MARTIN RIDAL,[b] AND OLE VIGNES[a]

[a] *Norwegian Meteorological Institute, Oslo, Norway*
[b] *Swedish Meteorological and Hydrological Institute, Norrköping, Sweden*
[c] *European Centre for Medium-Range Weather Forecasts, Reading, United Kingdom*

(Manuscript received 5 June 2016, in final form 15 December 2016)

ABSTRACT

Since October 2013 a convective-scale weather prediction model has been used operationally to provide short-term forecasts covering large parts of the Nordic region. The model is now operated by a bilateral cooperative effort [Meteorological Cooperation on Operational Numerical Weather Prediction (MetCoOp)] between the Norwegian Meteorological Institute and the Swedish Meteorological and Hydrological Institute. The core of the model is based on the convection-permitting Applications of Research to Operations at Mesoscale (AROME) model developed by Météo-France. In this paper the specific modifications and updates that have been made to suit advanced high-resolution weather forecasts over the Nordic regions are described. This includes modifications in the surface drag description, microphysics, snow assimilation, as well as an update of the ecosystem and surface parameter description. Novel observation types are introduced in the operational runs, including ground-based Global Navigation Satellite System (GNSS) observations and radar reflectivity data from the Norwegian and Swedish radar networks. After almost two years' worth of experience with the AROME-MetCoOp model, the model's sensitivities to the use of specific parameterization settings are characterized and the forecast skills demonstrating the benefit as compared with the global European Centre for Medium-Range Weather Forecasts' Integrated Forecasting System (ECMWF-IFS) are evaluated. Furthermore, case studies are provided to demonstrate the ability of the model to capture extreme precipitation and wind events.

## 1. Introduction

With the increasing resolution of operational numerical weather prediction (NWP) models toward kilometer scales, the direct simulation of small-scale features like convective dynamics is approached. This advancement provides weather services with the potential to improve short-term weather forecasts of convective events, which can have a severe impact on infrastructure and society at large. However, the progress in model resolution goes hand in hand with several challenges, for example, physical parameterization schemes, proper description of details in the surface forcing, and data assimilation of high-resolution data (e.g., Sun 2005). In addition, forecast evaluation becomes more complex (e.g., Ebert 2008) and underlines the fact that the gridpoint value itself from a high-resolution model is not necessarily the best end product.

In March 2014, the AROME-MetCoOp model, the Meteorological Cooperation on Operational Numerical Weather Prediction (MetCoOp) version of the Météo-France Applications of Research to Operations at Mesoscale (AROME) model (Seity et al. 2011), was put into operation by a cooperative effort of the Norwegian and Swedish meteorological services. MetCoOp, which is a collaborative effort between the Swedish Meteorological and Hydrological Institute (SMHI) and the Norwegian Meteorological Institute (MET-Norway), is unique in having two national weather services sharing operational model simulation, 24/7 surveillance, infrastructure (including computing resources), expertise, and model development. At present, MetCoOp produces short-term

*Corresponding author e-mail*: Malte Müller, maltem@met.no

DOI: 10.1175/WAF-D-16-0099.1

© 2017 American Meteorological Society. For information regarding reuse of this content and general copyright information, consult the AMS Copyright Policy (www.ametsoc.org/PUBSReuseLicenses).

www.manaraa.com

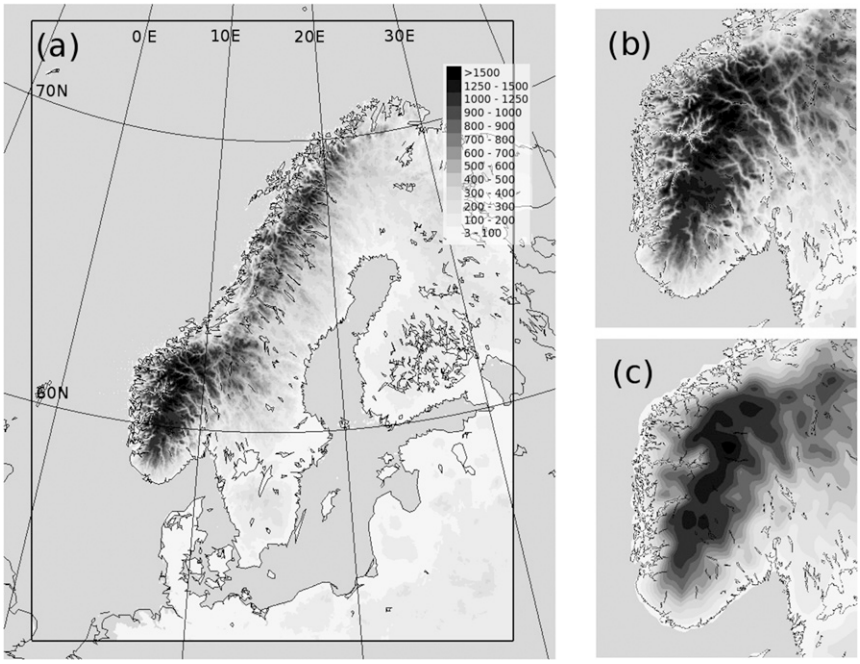


FIG. 1. Contoured land topography (elevation; m). (a) The entire model domain of the AROME-MetCoOp. A subarea (southern Norway) is shown of the (b) AROME-MetCoOp and (c) ECMWF-IFS topographies.

weather forecasts that are distributed and used in the forecast production chains of both countries. AROME-MetCoOp is a branch of the HIRLAM–ALADIN Research on Mesoscale Operational NWP in Euromed (HARMONIE) AROME model, version 38h1.2, which has been developed within the framework of the High Resolution Limited Area Model (HIRLAM) consortium (http://www.hirlam.org), a research cooperation of 11 European meteorological institutes.

Weather forecasting over Scandinavia spans a wide range of phenomena and scales and includes continental, maritime, and polar conditions. During summer, convective systems are common (in particular in the southeast), while polar processes, including severe polar lows, are frequently observed during winter (in the northern parts). Both Norway and Sweden have varying topography, complex coastlines, and gradients in land use, which imply local variations in weather. Thus, many aspects of weather forecasting in the Nordic region (Norway, Sweden, Finland, and Denmark) benefit from a better description of small-scale phenomena and forcing; that is, the topography, coastline, and land-use contrasts may steer temperature, wind, and precipitation gradients. In addition, severe weather, such as polar lows, is more likely to be simulated with kilometer-scale resolution, as a result of the improved representation of the smaller spatial scales of high-latitude dynamics (Kristiansen et al. 2011).

The scope of this paper is to introduce and evaluate the AROME-MetCoOp model after almost two years' worth of operation. The paper is structured as follows. Section 2 gives a brief description of the AROME-MetCoOp model and its configuration. Surface and upper-atmosphere data assimilation is outlined in section 3. In section 4, an evaluation is presented to show the general characteristics and added value of the AROME-MetCoOp model compared with the global European Centre for Medium-Range Weather Forecasts Integrated Forecasting System (ECMWF-IFS; Bauer et al. 2013). Case studies of severe weather events during the first operational year are described in section 5. The last section presents a summary along with future perspectives.

## 2. Model configuration and modifications

### a. *Model configuration*

The AROME-MetCoOp model covers large parts of the Nordic countries with a horizontal resolution of 2.5 km. More than half of its domain is over open water, that is, the Atlantic Ocean, the North Sea, and the Baltic Sea (Fig. 1). The horizontal grid (739 × 949 grid points) is defined by a Lambert projection with the center at 63.5°N and 15°E. The coupling zone in which the AROME-MetCoOp model is relaxed toward the large-scale coupling model is eight grid points wide

www.manaraa.com

(Davies 1976). In the vertical, the atmosphere is divided into 65 layers by a mass-based, terrain-following hybrid vertical discretization (Simmons and Burridge 1981). Near the ground, the first layer is at approximately 12.5-m height, and the vertical resolution decreases with height, with a discretization of 15–100 m in the lower 1 km of the atmosphere. The uppermost layer is located at approximately 33 km.

The model operates with a 3-hourly update cycling, where atmospheric and land surface variables are updated. At every main cycle (0000, 0600, 1200, and 1800 UTC) a 66-h forecast is produced. For these main cycles the cutoff time, the waiting time after the official analysis for observations, is 1 h 15 min. For the intermediate cycles (0300, 0900, 1500, and 2100 UTC), a very short-term forecast of 3 h is produced and used as a background field for the following main cycle. The cutoff time for the intermediate cycles is 3 h 40 min.

The AROME-MetCoOp model is forced by ECMWF-IFS at the lateral and upper boundaries. The ECMWF-IFS model operates with a T1279 horizontal resolution (approx 16-km grid size) and 137 vertical levels. Because of the delayed availability of ECMWF-IFS forecasts, the analysis times of the ECMWF-IFS forecasts, which are used as boundaries, are 3 and 6 h earlier than the actual forecast for the intermediate and main forecast cycles, respectively.

### b. *Modifications in the microphysical scheme*

In the following we give a brief description of the cloud microphysics scheme, where region-specific adjustments have been made. For a detailed description of the model numerics and physics, we refer readers to Seity et al. (2011) and references therein.

The cloud microphysics is based on a Kessler scheme for the warm (liquid) processes whereas the cold processes are parameterized by the three-class ice parameterization (ICE3) scheme. ICE3 includes three ice species; cloud ice, snow, and graupel (Pinty and Jabouille 1998). More than 25 processes are parameterized inside the scheme and most of them are interactions between different species. Those processes are treated explicitly and sequentially, and the result is dependent on the order of the calculation of each process. Altogether six species are used: vapor, cloud water, rain, cloud ice, snow, and graupel. They are all advected horizontally by the semi-Lagrangian scheme. The gravitational settling of non-vapor water is parameterized by a sedimentation scheme, which is designed to be both numerically stable and computationally efficient. Subgrid condensation is accounted for by a statistical subgrid condensation scheme. The cloud fraction of a grid box with a nonsaturated mean of vapor is determined by the averaged departure of saturation and of the variance of the departure from saturation. This variance is diagnosed by the output from the turbulence scheme.

The modifications of the ICE3 scheme for AROME-MetCoOp are motivated by the following weaknesses seen during the winter season:

- too quick decay of low clouds in cold conditions (e.g., 2-m temperatures $T_{2m}$ from about −5° to −10°C), which leads to too large longwave outgoing radiation and thus too low $T_{2m}$, and
- too much ice fog or low clouds in severe cold conditions ($T_{2m}$ about −15°C or colder). There also seems to be a slight overprediction of cirrus clouds. This overprediction is present in all seasons.

The modifications include

- separating the fast liquid-phase processes from the slower ice-phase processes,
- reducing the speed of the sublimation of ice particles, and
- accounting for the fact that the optical thickness of ice-phase clouds is less than the optical thickness of water- or mixed-phase clouds.

These modifications reduce the negative bias of $T_{2m}$ in winter and improve the low-level cloudiness. A negative side effect is that the occasions with fog increase and become too frequent. The reason for this is that during winter and spring the latent heat transport in the surface scheme is too large and the sensible heat flux too low. Without the modifications in the microphysics, the effect of this error in the surface scheme is partly compensated by a too rapid precipitation release from the lowest clouds, including fog.

In the following, we present a 24-day sensitivity experiment during a cold winter period. The reference experiment and a sensitivity experiment, with the above outlined modifications in the microphysics scheme, are verified against cloud-base observations from 38 Swedish automatic stations (Fig. 2). First, the frequency bias (definition see section 4) for different cloud-base classes shows that the lowest cloud base (including fog) is too frequent in the reference version. This is also the case for the second highest cloud class (1500–4000-m height), which is mostly a secondary effect of the underprediction of low clouds. The modified version has a frequency bias closer to one, although there are still some systematic errors. Other experiments showed that all three of the ICE3 modifications contribute to the reduction of frequency bias. Furthermore, they showed that accounting for the lower optical thickness of ice-phase clouds is especially important for the reduction of (ice) fog. The amount of cirrus clouds is generally lower

www.manaraa.com

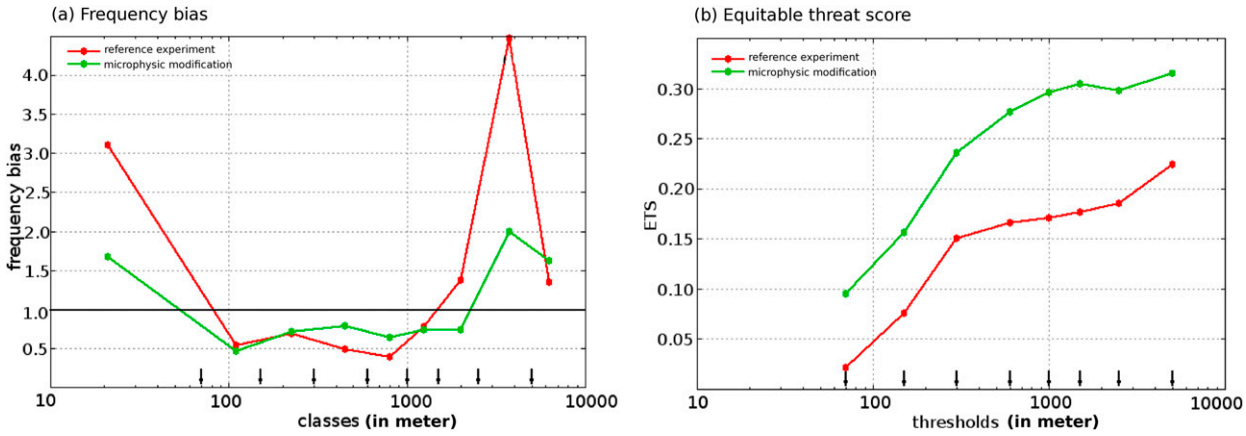


FIG. 2. A 24-day sensitivity experiment with modifications in the microphysics scheme as described in the text. The reference experiment (red) and the modified version (green) are shown. (a) The frequency bias for different cloud-base classes. A class is defined by a range of heights (m) above the surface, e.g., the highest cloud-base class also includes clear sky and clouds above 7500 m. The ideal frequency bias equal to one is indicated by a solid line. (b) The ETSs for different thresholds of cloud-base heights (m).

with the modified version, which seems to be better from a subjective perspective. It is difficult to objectively verify this, since the treatment of thin cirrus is doubtful, and the automatic stations are only able to detect clouds up to 7.5 km.

The equitable threat scores (defined in section 4) for different thresholds of cloud base show that the modifications of the microphysics scheme improve the skill in all cloud-base thresholds (Fig. 2b). In summer there is only a small and nearly neutral effect of the updates (not shown). A positive side effect is that the overprediction of very high precipitation amounts (seen mostly in summer) is reduced. The reason for this is not obvious, but the separation of liquid-phase processes from the slower ice-phase processes may slow down the speed of the modeled total precipitation production.

### c. *The surface model*

Interactive atmosphere–surface and surface–soil processes are described by the Surface Externaliseé (SURFEX) model (Masson et al. 2013). SURFEX includes routines designed to simulate the exchange of energy and water between the atmosphere and four surface types (tiles): land, ocean, inland water, and town. The fluxes computed by SURFEX at the atmosphere–surface interface serve as the lower boundary conditions for the atmospheric part of the model. All surface processes are treated as one-dimensional vertical processes, with different options for specifying the required degree of physical complexity.

The land surface parameters are defined by the ECOCLIMAP 1-km resolution global database (Masson et al. 2003), which initializes the soil–vegetation–atmosphere transfer schemes in the surface model. In the initial phase of operating a convective-scale weather prediction system, the ECOCLIMAP1 database (Masson et al. 2003) was used and replaced in May 2013 by the new version, ECOCLIMAP2 (Faroux et al. 2013). The introduction of the ECOCLIMAP2 physiography had a significant impact on the model's performance. The main motivation for changing to ECOCLIMAP2 was in addressing the problematic features of ECOCLIMAP1 in some parts of the model domain. For example, the surface roughness was too low, which led to too high wind speeds in Trøndelag, in the middle of Norway. Also, in ECOCLIMAP1 large parts of southern Norway are given, by mistake, the surface type "permanent snow." ECOCLIMAP2 gives more realistic roughness values in Trøndelag and a more realistic extent of the permanent snow in the model domain. Furthermore, there is a general increase and modification of the seasonal cycle in the leaf area index (LAI) in the new ECOCLIMAP2 version. The LAI directly impacts the surface roughness in the surface boundary layer modeling (SBL) within SURFEX.

The SBL scheme is a one-dimensional prognostic turbulence model. The exchange of momentum and heat with the surface is a function of the surface roughness, on land tiles calculated from the LAI and vegetation height. Additional "canopy drag" is activated, increasing the drag within the SBL as a function of LAI and vegetation fraction, and thereby reducing the wind speed. It is possible to also add orographic drag, but that option is not used in the current setup of AROME-MetCoOp.

Donier et al. (2012) realized that the most important effect of the change from ECOCLIMAP1 to ECOCLIMAP2, when evaluating the performance of AROME-France, was induced by an increased seasonal

www.manaraa.com

cycle of LAI. Our findings are consistent with those of Météo-France in that it had a strong impact on the forecast skills of 2-m relative humidity $RH_{2m}$, as well as $T_{2m}$. Specifically, summer nighttime $T_{2m}$ was overestimated and $RH_{2m}$ underestimated. It was found that the reason for that was too stable stratification in some situations. To prevent too stable stratification, the maximum Richardson number $Ri_{max}$ was reduced from 0.2 to 0.0, leading to significantly improved forecast skill (see also Donier et al. 2012).

In areas with vegetation, the change from ECOCLIMAP1 to ECOCLIMAP2 also affected the wind speed and led to an underestimation of $U_{10m}$. Sensitivity experiments have shown that a reduction in the tuning coefficient of the canopy drag (from 0.05 to 0.01) leads to more realistic wind speeds in vegetation-covered areas, and moreover, improved the performance in stable summer nights with respect to $T_{2m}$ and $RH_{2m}$. This is illustrated by a sensitivity experiment, where the canopy drag and Richardson number are reduced, over a 15-day period during summer 2011 (Fig. 3). The forecasts of $T_{2m}$ and $U_{10m}$ are evaluated against observations from Norwegian and Swedish synoptic stations. The mean errors of the $T_{2m}$ and $U_{10m}$ forecasts are significantly reduced, consistent with the preceding explanation.

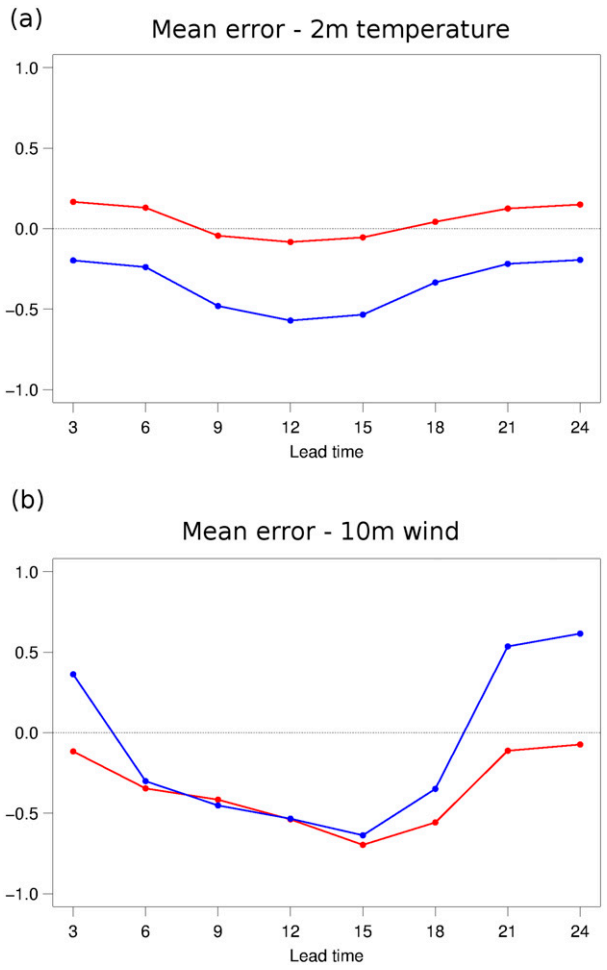


FIG. 3. A 14-day sensitivity experiment with modifications in the surface model (reduced canopy drag and Richardson number), as described in the text. The reference experiment (blue) and the modified version (red) are shown. The mean errors for (a) 2-m temperature and (b) 10-m wind speed are shown.

## 3. Data assimilation

### *a. Surface data assimilation*

The surface analysis is performed by Code d'Analyze Nécessaire à ARPEGE pour ses Rejets et son Initialization (CANARI; Taillefer 2002), using conventional synoptic observations of $T_{2m}$, $RH_{2m}$, and snow depth from synoptic and climatological stations (Fig. 4). The analysis method is optimal interpolation (OI), in which surface temperature, soil temperature, and moisture fields are updated, based on $T_{2m}$ and $RH_{2m}$ analysis increments. In Fig. 5a the network of surface observation stations in the MetCoOp area are visualized.

Snow cover is modeled by a one-layer scheme with three prognostic variables: snow water equivalent (SWE), snow density, and snow albedo. The conversion of snow-depth observations to SWE in CANARI is based on climatological monthly mean snow density values ranging from $143\,kg\,m^{-3}$ (in autumn) to $312\,kg\,m^{-3}$ (in spring). The influence of the observations is a function of both horizontal and vertical distance and is adapted to the Nordic network of snow-depth observations (Homleid and Killie 2013). Most of the snow-depth observations are only available at 0600 or 1800 UTC, and accordingly the snow analysis is only performed twice daily with the first guess from a 3-h forecast from the previous cycle. The assimilation of snow depths leads to an improvement in the simulation of the snow depth, especially during the melting season in spring (Homleid and Killie 2013).

The sea surface temperature (SST) is taken from the ECMWF-IFS, which, in turn, provides a product based on the Met Office's Operational Sea Surface Temperature and Sea Ice Analysis (OSTIA; Donlon et al. 2012). Sea ice concentrations are obtained from the Ocean and Sea Ice Satellite Application Facilities (OSI-SAF) from MET-Norway. Also, the surface temperature over sea ice is taken from the ECMWF-IFS and remains unchanged throughout the forecast. There are ongoing efforts to improve the SST and sea ice concentration representations in the model and, further, to provide for coupled atmosphere–ocean forecasts with a one-dimensional ocean model approach (Brossier et al. 2009).

www.manaraa.com

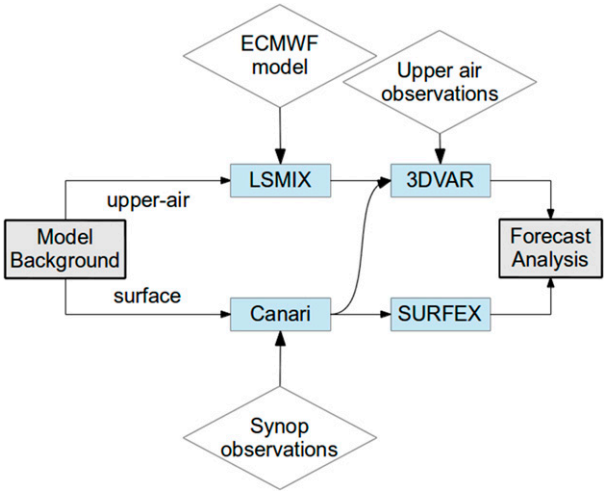


FIG. 4. Sketch of the surface and upper-air data assimilations. Upper-air variables are updated by spectral mixing of the host model information (LSMIX) and performing a 3DVAR data assimilation of observations (synoptic stations, drifting buoys, aircrafts, radiosondes, GNSS ZTD, radar, and satellites). The surface fields are updated by OI (CANARI). Furthermore, the surface processes are simulated by SURFEX.

### b. *Spectral mixing*

The upper-air forecast analysis is obtained by mixing in large-scale information (LSMIX) of the ECMWF-IFS and by three-dimensional variational (3DVAR) data assimilation of observations into the model background (Fig. 4). The model background is a 3-h forecast from the previous cycle. With LSMIX, large-scale information from the host model is transferred, in a simplified form, into the limited area high-resolution model (Guidard and Fischer 2008; Dahlgren and Gustafsson 2012). For all spectral control variables the ECMWF-IFS forecast $\mathbf{x}_h$ valid at the analysis time is mixed in the model background $\mathbf{x}_b$ by

$$\tilde{\mathbf{x}}_b(m,n,l) = w(m,n,l)\cdot\mathbf{x}_h(m,n,l) + [1-w(m,n,l)]\cdot\mathbf{x}_b(m,n,l). \quad (1)$$

where $(m, n)$ refer to the horizontal wavenumbers, $l$ is the vertical model level, and $w(m, n, l)$ is the weighting function. A detailed description of LSMIX is given in the appendix. In principle the LSMIX approach is similar to the spectral nudging technique used for dynamical downscaling of global climate model output (Von Storch et al. 2000). In the present AROME-MetCoOp operational system, the weighting function is separated in $w(m, n, l) = u(m, n)v(l)$, where the vertical weighting function $v(l)$ is a simple polynomial and the horizontal weighting function $u(m, n)$ is described by a step function. With an improved representation of the weighting

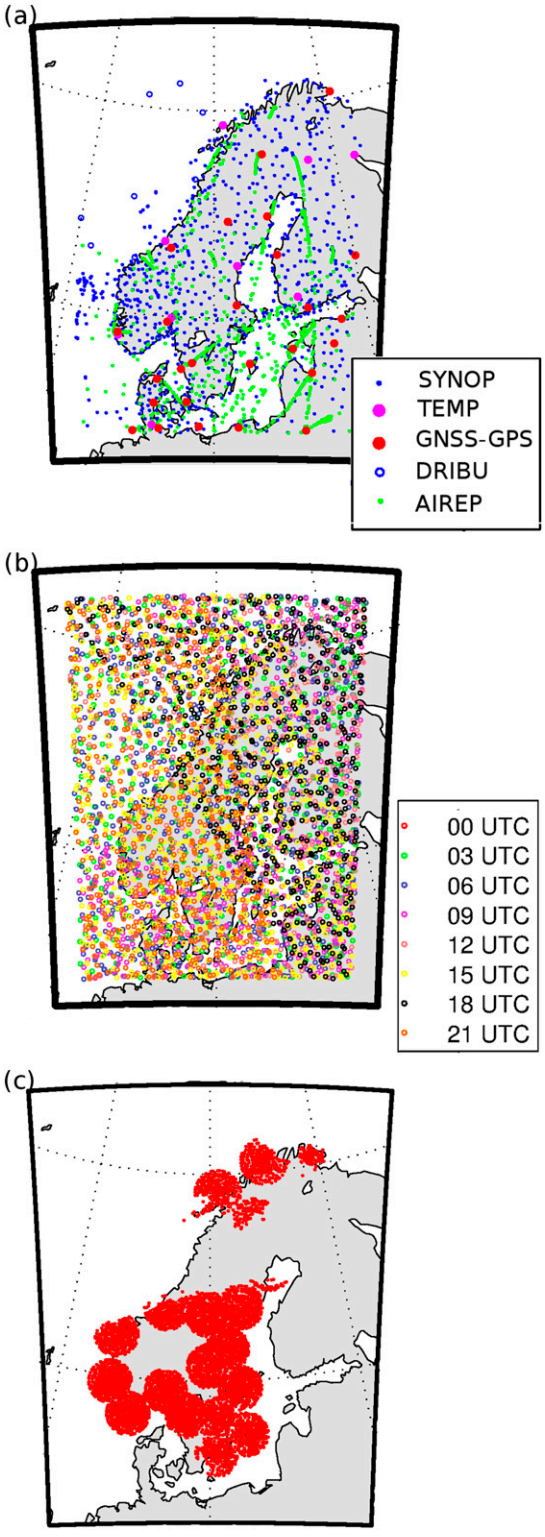


FIG. 5. Observational data used in the 3DVAR data assimilation. (a) Snapshot (1200 UTC 2 Sep 2015) of conventional observations, (b) daily cycle of ATOVS observations (2 Sep 2015), and (c) all radar reflectivity observations on 2 Sep 2015.

www.manaraa.com

function in the form of an error covariance matrix, LSMIX would be equivalent to the $J_k$ term formulation (Dahlgren and Gustafsson 2012). This equality is shown in the appendix. The LSMIX approach has a significant positive impact on forecasts of upper-air temperature (verified against radiosondes) and on mean sea level pressure (Dahlgren 2013).

### c. Upper-air data assimilation

In the AROME upper-air 3DVAR data assimilation system (Fig. 4), the background-error covariances use a multivariate formulation based on the forecast errors of the control variables (i.e., vorticity, divergence, temperature, surface pressure and specific humidity errors) (Berre 2000). The background error covariance matrix (**B** matrix) is computed with the assumption of horizontal spatial homogeneity and isotropy. These assumptions allow for a number of simplifications in the representation of the **B** matrix and the minimization procedure of the cost function (Berre 2000). In the operational model setup we use a "climatological" representation of the **B** matrix and do not take into account any time dependence (Brousseau et al. 2012) nor heterogeneous information in space (Montmerle and Berre 2010).

At the current stage, conventional observations from surface synoptic stations[1] (SYNOP), drifting buoys (DRIBU), aircrafts (AIREP), and radiosondes (TEMP) are used in the 3DVAR upper-air data assimilation system (Fig. 5a). Furthermore, satellite radiance observations from three Advanced TIROS Operational Vertical Sounders (ATOVS), Global Navigation Satellite System (GNSS) zenith total delay (ZTD) observations, and radar reflectivity from the Norwegian and Swedish radar networks are assimilated. In the following, we briefly discuss the assimilation strategies for GNSS ZTD, ATOVS, and radar reflectivity observations.

From ATOVS instruments, the Advanced Microwave Sounding Unit (AMSU-A and AMSU-B) and the Microwave Humidity Sounder (MHS) data are processed at their full resolution (Randriamampianina 2006). The different biases of the satellite data are corrected by using an adaptive variational scheme (Dee 2005). The coefficients for the bias correction are aggregated daily for each assimilation time and are compared to the continuous cycling updates of the global model forecast system (Randriamampianina et al. 2011). The data are thinned with an average resolution of 80 km. An example of the data coverage for all cycles for a specific day is shown in Fig. 5b.

The GNSS ZTD provides information of columnar water vapor and results are obtained through the Network of European Meteorological Services (EUMETNET) global positioning system (GPS) Water Vapor Program, which is a collaborative effort between the European geodetic community and several European national meteorological institutes. At present we make use of GNSS ZTD observations from the Met Office and the Royal Meteorological Institute of Belgium processing centers, who provide around 20 stations for our domain (Fig. 5a). In the near future, it is planned to have access to around 600 stations by a data-processing infrastructure. A novel aspect of our GNSS ZTD is the operational use of a variational bias correction to adaptively handle biases in the GNSS ZTD observations. For a detailed description and analysis, we refer to Sánchez Arriola et al. (2016).

Quality controlled radar reflectivity results from the Norwegian and Swedish radar network are assimilated (Fig. 5c). The reflectivity data are filtered to a resolution of 15 km by selecting one-dimensional reflectivity profiles within 15 km × 15 km boxes. Then, a 1D Bayesian estimate of a relative humidity profile is retrieved from the reflectivity and, subsequently, assimilated within the 3DVAR approach following the strategies described in Caumont et al. (2010) and Wattrelot et al. (2014). Note that the quality control process of the radar reflectivity data distinguishes between areas of no rain and no observations. Thus, observations of no rain are also considered in the data assimilation system. The impact of radar data assimilation on the forecast of $RH_{2m}$ is illustrated in Fig. 6. It is a 2-week experiment that took place during May 2015, and the impact of the assimilation of reflectivity data from the entire Norwegian and Swedish radar network is tested. The result illustrates a small positive impact on the forecast of relative humidity on forecast lengths up to 24 h. Verification of relative humidity against radiosonde observations shows a similarly small improvement below 500-hPa height, in addition to a forecast degradation at 700 hPa (not shown). The latter is not understood, so far, and remains part of our ongoing work.

## 4. Evaluation of the model

### a. Evolution of the model system

There has been an active development of the HARMONIE-AROME model in recent years within the HIRLAM consortium. At the Norwegian Meteorological Institute the HARMONIE-AROME model has been in use since May 2011, and a timeline of model

[1] Only surface pressure is used in the upper-air data assimilation system.

www.manaraa.com

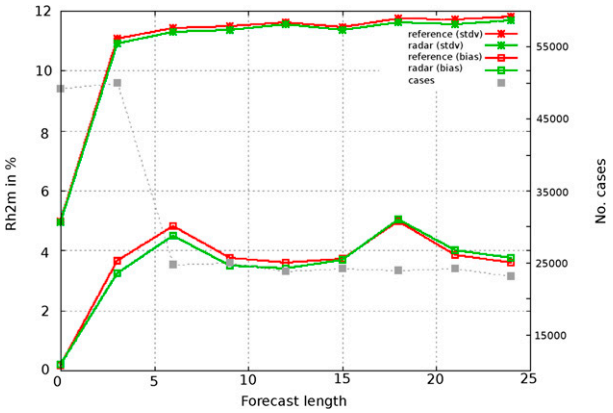


FIG. 6. The 14-day data-denial experiments without (red) and with (green) data assimilation of radar reflectivities from the Norwegian and Swedish radar networks. The impact on 2-m relative humidity observations is shown. The *y* axis represents the root-mean-square error and bias (for red and green curves) and shown in gray is the number of cases in the verification process. The *x* axis represents the lead time (h) of the forecast.

changes and updates is illustrated by the monthly standard deviation of the error and bias of temperature assessed for 154 Norwegian stations (Fig. 7). Note that the model changes and different versions are not referring solely to modifications done by the Norwegian MET service, but are also the result of combined efforts within HIRLAM. The AROME model was running in an experimental mode (Harmonie2.5), which in November 2012 became the AROME-Norway model. Those models were without 3DVAR data assimilation, based on AROME physics (Seity et al. 2011), and operated on similar domains as AROME-MetCoOp. In June 2013, the AROME-Norway model (based on HARMONIE-AROME version 37h1.2) became operational and has been used as the main weather forecast model for Norway from October of the same year. Major modifications and improvements were performed in 2013, when the ECOCLIMAP1 map was replaced by ECOCLIMAP2. As described in section 2c, this resulted in model performance issues. The required adjustments to the surface drag and the maximum Richardson number followed in November 2013. In March 2014 the AROME-MetCoOp model (based on HARMONIE-AROME version 38h1.1) became operational. The microphysics were modified, as described in section 2b, during December 2014 (HARMONIE-AROME version 38h1.2).

The verification of $T_{2m}$ of almost 4 yr shows a reduction in the standard deviation error for the ECMWF-IFS and the AROME model systems during winter. Thus, in the second half of the time series, the evaluation of the ECMWF-IFS and AROME-MetCoOp models shows less variability in between seasons. The temperature mean error developments differ in time. AROME-MetCoOp has a warm winter bias in 2011 and 2012, which changes to a cold winter bias in the following years, after the change to ECOCLIMAP2, which reduced the surface drag and changed the maximum Richardson number. Furthermore, in the first half of the time series ECMWF-IFS always has slightly smaller or equal standard deviations of error compared with AROME-MetCoOp, while the results are of similar size in the second half. During the entire period AROME-MetCoOp has fewer systematic deviations than ECMWF-IFS.

### b. One-year evaluation

The performance of the AROME-MetCoOp model is presented over a period of 12 months ranging from 1 September 2014 to 31 August 2015. Quality controlled synoptic observations of 10-m wind speed $U_{10m}$, 2-m temperature $T_{2m}$, and 12-h accumulated precipitation RR12 from the Norwegian and Swedish observation network are used for the evaluation. The forecast skill of the AROME-MetCoOp model is compared against that of the global ECMWF-IFS with a specific focus on lead times ranging from 6 to 30 h.

The mean absolute error (MAE) and the corresponding skill score $s_{MAE}$, defined as

$$s_{MAE} = 1 - \frac{MAE_{AROME}}{MAE_{ECMWF}}, \tag{2}$$

are used to evaluate the forecast skill of precipitation, temperature, and wind (Figs. 8 and 9). Note that $s_{MAE}$ is only shown for the temperature forecast evaluation. The forecasts of precipitation and wind are further assessed (Fig. 10) by using the equitable threat score (ETS),

$$ETS = \frac{a - a_r}{a + b + c - a_r} \quad \text{and} \tag{3}$$

$$a_r = (a + b)(a + c)/N, \tag{4}$$

and the bias frequency (BF),

$$BF = \frac{a + b}{a + c}. \tag{5}$$

Here, $N$ is the length of the sample ($N = a + b + c + d$) and the events $a$, $b$, $c$, and $d$ are given in a contingency table (Table 1).

#### 1) TEMPERATURE

The largest improvements in temperature forecasts, where $s_{MAE}$ values are larger than 0.3, are seen in Norway, and in particular in the mountainous regions (Fig. 8). There, the main contribution to the improved forecast skill is due to better resolution of topography in

www.manaraa.com

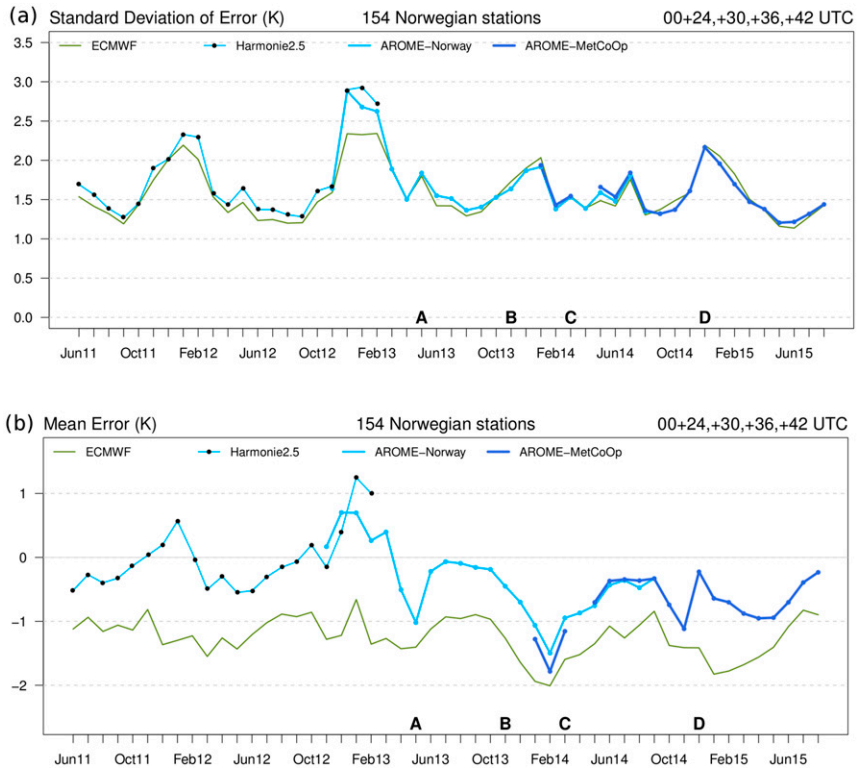


FIG. 7. The (a) standard deviation error and (b) mean error (K) of 2-m temperature computed for 154 Norwegian synoptic stations. The evaluation ranges from June 2011 to August 2015. It includes the ECMWF-IFS for the whole time period, and three high-resolution AROME model setups used within the last 4 yr: Harmonie2.5, AROME-Norway, and AROME-MetCoOp. Major milestones in the establishment of AROME as an operational weather prediction model are indicated by letters A–D, where A is the change from ECOCLIMAP1 to ECOCLIMAP2 (27 May 2013), B is the reduced drag and change of maximum Richardson number (4 Nov 2013), C is when AROME-MetCoOp became operational (12 Mar 2014), and D is the change from cy38h1.1 to cy38h1.2 (8 Dec 2014).

the AROME-MetCoOp model compared with the ECMWF-IFS.[2] The AROME-MetCoOp resolution is sufficient to resolve to a great degree the Norwegian mountains and fjords. In the Norwegian coastal areas and in the flat-topography regions in Sweden improvements from using a higher-resolution model are present, but more modest. Generally, the ECMWF-IFS model has a negative temperature bias in winter over the entire domain (see also Fig. 7b). The AROME-MetCoOp model is capable of reducing this bias, except for in some parts in northern Sweden, where the $s_{MAE}$ score is around zero year-round.

In the temperature MAE a characteristic seasonal cycle with MAE values of more than 2.5° in wintertime is present for the ECMWF-IFS (Fig. 9a; see also Fig. 7b). This seasonality is significantly reduced in the AROME-MetCoOp model to values smaller than 1.8° in the Norwegian area. The increased errors during winter can be partly explained by the complexity of temperature forecasting within cold winter surface and local inversion situations, compared with summer conditions where the sun is the dominant driver of the near-surface temperature. In Sweden, the temperature MAE is smaller than in Norway and the two models are almost identical, except for during winter when AROME-MetCoOp has a smaller temperature bias than ECMWF-IFS. Note that during December 2014 the model version was updated, which included the improvements in the microphysic scheme described in section 2b and effectively reduced the winter temperature bias.

### 2) PRECIPITATION

The MAE for RR12 is improved mainly in Norway, where orographically forced precipitation is the dominant

[2] See also Figs. 1b and 1c, where the topographies of the two model systems are shown for a mountainous area in Norway.

www.manaraa.com

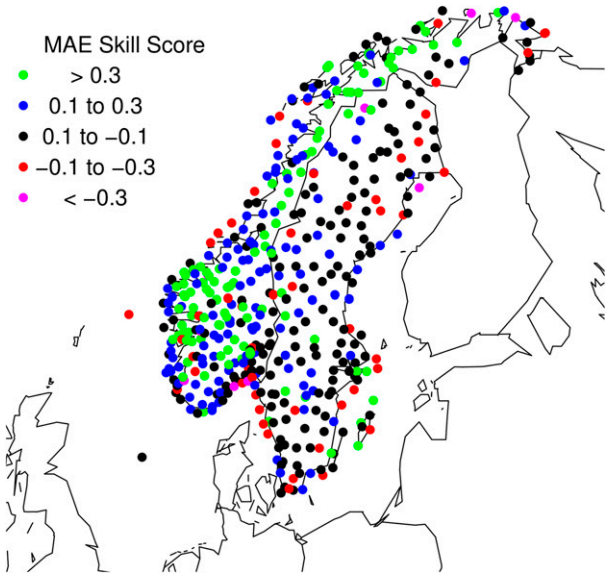


FIG. 8. MAE skill score for temperature for forecast lead times from 6 to 30 h averaged over a 1-yr period from September 2014 to August 2015.

mechanism. There, the high resolution of the AROME-MetCoOp model has a positive impact. Over Sweden, where convective precipitation is a dominant mechanism, the MAE values are similar between the two models (Fig. 9b). The precise forecast of convective cells is challenging, and thus, a point verification method is problematic for those small-scale features. A well-forecasted precipitation amount, but mislocated by a few kilometers, can lead to a "double penalty" and thus to a reduced skill score. Hence, we will use a spatial verification method, the fractional Brier skill score (FBSS; Roberts and Lean 2008), to monitor the capability of the two different models to predict the probability of precipitation over certain threshold values and for different area sizes. Often radar information is used for FBSS analysis, but since our current radar products are not accurate enough, we analyzed a dense network of rain gauges within the MetCoOp domain for a period of 9 months (October 2014–June 2015) and considered forecast lengths from 6 to 30 h. The reference forecast is the observed frequency of occurrence of precipitation exceeding the different thresholds.

For FBSS calculations the model domain is subdivided into squares of varying size, measured in degree latitude and longitude (1° is ≈ 111 km). Only squares with at least three observations are considered in the analysis. In Fig. 11 the FBSS values for different precipitation thresholds and square sizes are shown. For all thresholds and square sizes, FBSS values for AROME-MetCoOp are positive and larger than for the ECMWF-IFS. Most apparent are the differences between the two models for small thresholds (0.1 mm) and for large thresholds (20 and 35 mm). Thus, the spatial verification implies that the occurrence of strong precipitation events is generally better captured with the higher-resolution model. A consistent, but less significant, result is obtained for the ETS in Norway for small (<5 mm) and large (>15 mm) precipitation (Fig. 10). In the range between 5 and 15 mm in Norway and in general, for precipitation in Sweden, the ETS score is slightly larger for ECMWF-IFS than for AROME-MetCoOp. Compared with the results of the FBSS score, this illustrates the double-penalty issue when using point verification for high-resolution models in areas where orographically forced precipitation is less dominant.

The analysis of the BF also suggests that in Sweden the AROME-MetCoOp model is able to simulate the precipitation amounts more realistically than the ECMWF-IFS. Precipitation events smaller than approximately 10 mm have a BF larger than 1, which means that both models overestimate the occurrence of those events. In particular, ECMWF-IFS over Norway shows large BF values of up to 1.5. For precipitation amounts larger than 15 mm, the ECMWF-IFS has values around 0.5 over Norway and, thus, only 50% of those events are forecasted. For the Swedish region the AROME-MetCoOp has a BF close to 1 and for the ECMWF-IFS underestimates the frequency of large precipitation events, shown by BF values of around 0.5.

### 3) WIND

AROME-MetCoOp has in the entire model domain a smaller MAE for wind than does ECMWF-IFS (Fig. 9c). There is only a 2-month period in winter when the ECMWF-IFS shows smaller MAE values for the Swedish area. Furthermore, the ETS and BF values for wind confirm the good performance of the AROME-MetCoOp model for all wind speeds (Fig. 10). ECMWF-IFS performance is best in the range of winds speeds from about 4 to 10 m s$^{-1}$ with ETS values of around 0.4. For wind speeds larger than 10 m s$^{-1}$ the BF is smaller than 0.5 and, thus, the global forecasting system misses more than 50% of those strong wind events. Instead, AROME-MetCoOp shows, for wind speeds in the range of 3–13 m s$^{-1}$, ETS values larger than 0.4 and BF values of around 1. The BF drops below 0.5 for wind speeds larger than around 18 m s$^{-1}$.

In summary, we find that the AROME-MetCoOp model improves wind, temperature, and precipitation forecasts compared with the ECMWF-IFS. In the areas with complex topography (e.g., the Norwegian mountains) the high-resolution model adds considerable value to the temperature and wind forecasts. Large wind

www.manaraa.com

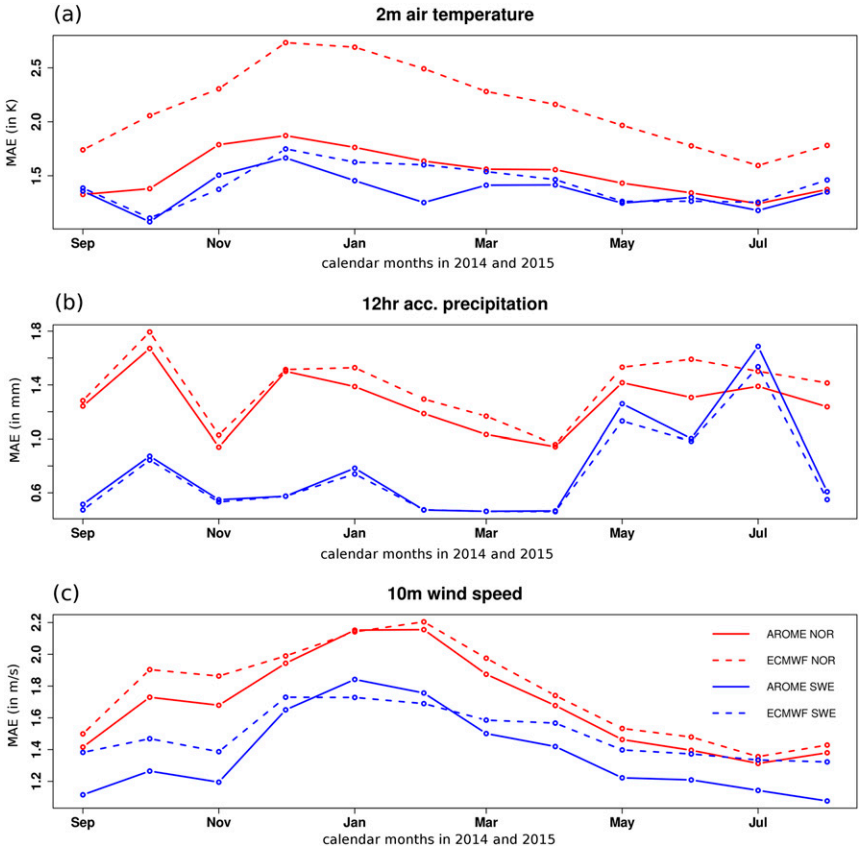


FIG. 9. Monthly averages of MAE subdivided into the Norwegian (red) and Swedish (blue) parts of the domain. MAEs are shown for the period from September 2014 to August 2015 for the ECMWF-IFS (dashed lines) and AROME-MetCoOp (solid lines) model forecasts with lead times from 6 to 24 h. The errors in (a) 2-m temperature, (b) 12-h accumulated precipitation, and (c) 10-m wind are assessed.

speeds and precipitation amounts are also significantly better simulated by the AROME-MetCoOp model.

## 5. Extreme weather case studies

### *a. Summer convective events in southern Sweden*

In August 2014 several heavy-precipitation events occurred across southern Scandinavia. Locally, severe damage was reported. We will focus on the 24-h period from 0600 UTC 19 August to 0600 UTC the following day. During this period southern Sweden experienced moist southwesterly winds associated with heavy rain showers and the mean sea level pressure (MSLP) map (not shown) is dominated by a low pressure center off the coast of mid-Norway.

The AROME-MetCoOp and ECMWF-IFS forecasts of 24-h accumulated precipitation are shown in Figs. 12a and 12b with maximum values given by numbers. An area of particularly intense precipitation associated with a trough is found in both models. Over a region in southern Norway (Figs. 12c,d), south of Lake Vaenern and 20 km north of Gothenburg, more than 80 mm of rain within 12 h was reported from rain gauge stations. Several stations measured more than 100 mm over the 24-h period (observed precipitation amounts are marked by colored squares in Figs. 12c–e). In the AROME-MetCoOp forecast the area of intense precipitation is considerably larger and extends much further inland, compared with the forecast of ECMWF-IFS, which has its largest precipitation amounts along the coast. Furthermore, local maxima of convective precipitation to the north of Lake Vaenern were forecasted by AROME-MetCoOp only. In general, all maxima are higher in the Arome-MetCoOp forecasts.

The forecasts from AROME-MetCoOp are in better agreement with the rain gauge measurements and also with the radar products for the areas with large precipitation amounts. Both the extension of the

www.manaraa.com

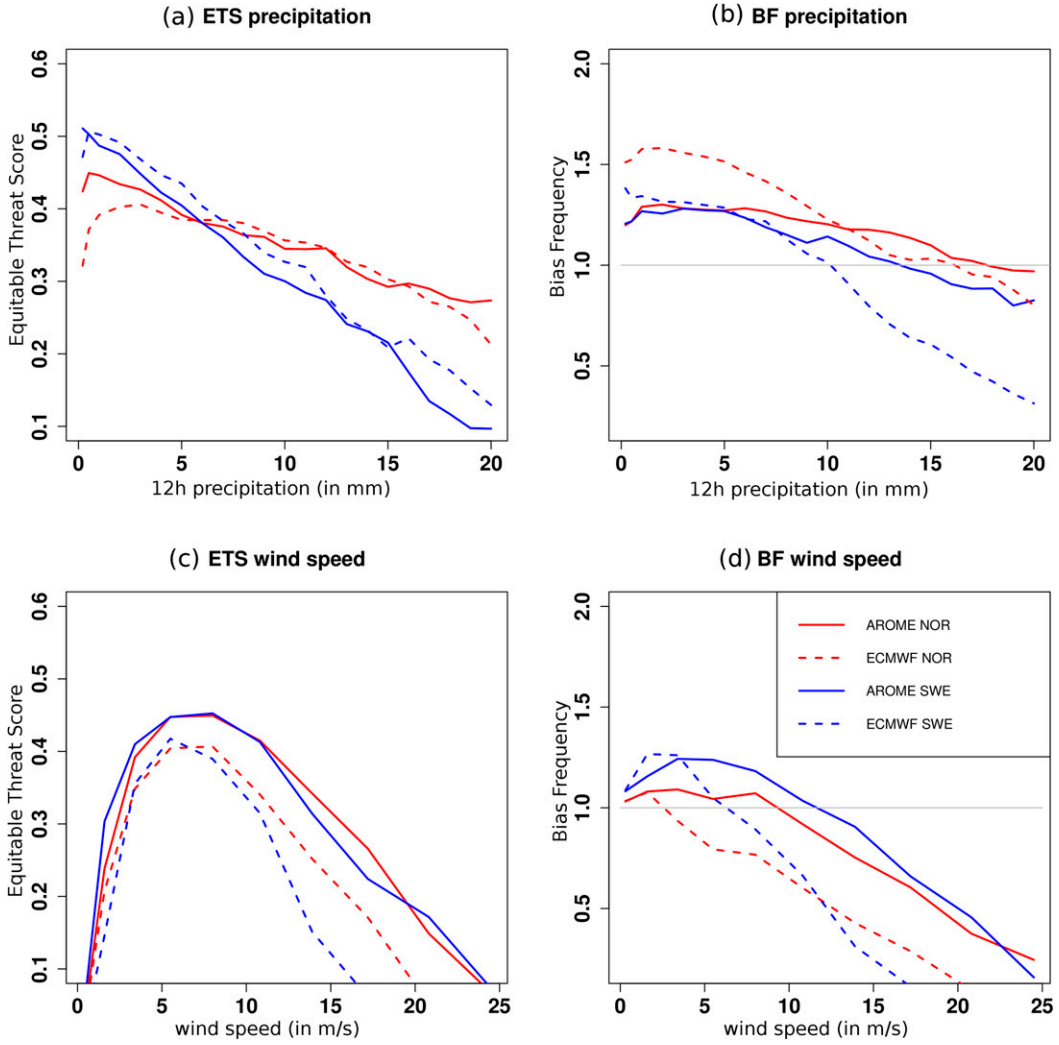


FIG. 10. (left) ETS and (right) BF for (a),(b) 12-h accumulated precipitation and (c),(d) wind speed computed for the period from September 2014 to August 2015. The computation is subdivided into the Norwegian (red) and Swedish (blue) parts of the domain and forecasts from the ECMWF-IFS (dashed lines) and AROME-MetCoOp (solid lines) models are assessed.

maximum area inland and the smaller amounts along the coast from this model is in better agreement with the measurements. The aforementioned small-scale convective cells north of Lake Vaenern are visible in the radar product and are indicated by some high values observed at rain gauges. The estimation given by the radar product should, however, be interpreted with some care as the radar beam is about 6 km above the ground at this distance from the radar site. When looking more closely, it becomes evident that although the AROME-MetCoOp model captures the locations of some areas of heavy precipitation better, the model still underestimates the observed maxima. Some areas with large precipitation amounts are missing in the forecasts, and peak values are not exactly collocated with the observed results. Thus, this suggests that for convective precipitation the use of an ensemble prediction system for forecasting rainfall probabilities could be advantageous.

### b. *Strong rainfall in western Norway*

At the end of October 2014, multiday heavy rainfall in the western parts of Norway caused severe flooding and led to significant infrastructure damage. The hourly

TABLE 1. Contingency table used for the calculation of ETS.

| | Observed yes | Observed no |
|---|---|---|
| Forecasted yes | *a* | *b* |
| Forecasted no | *c* | *d* |

www.manaraa.com

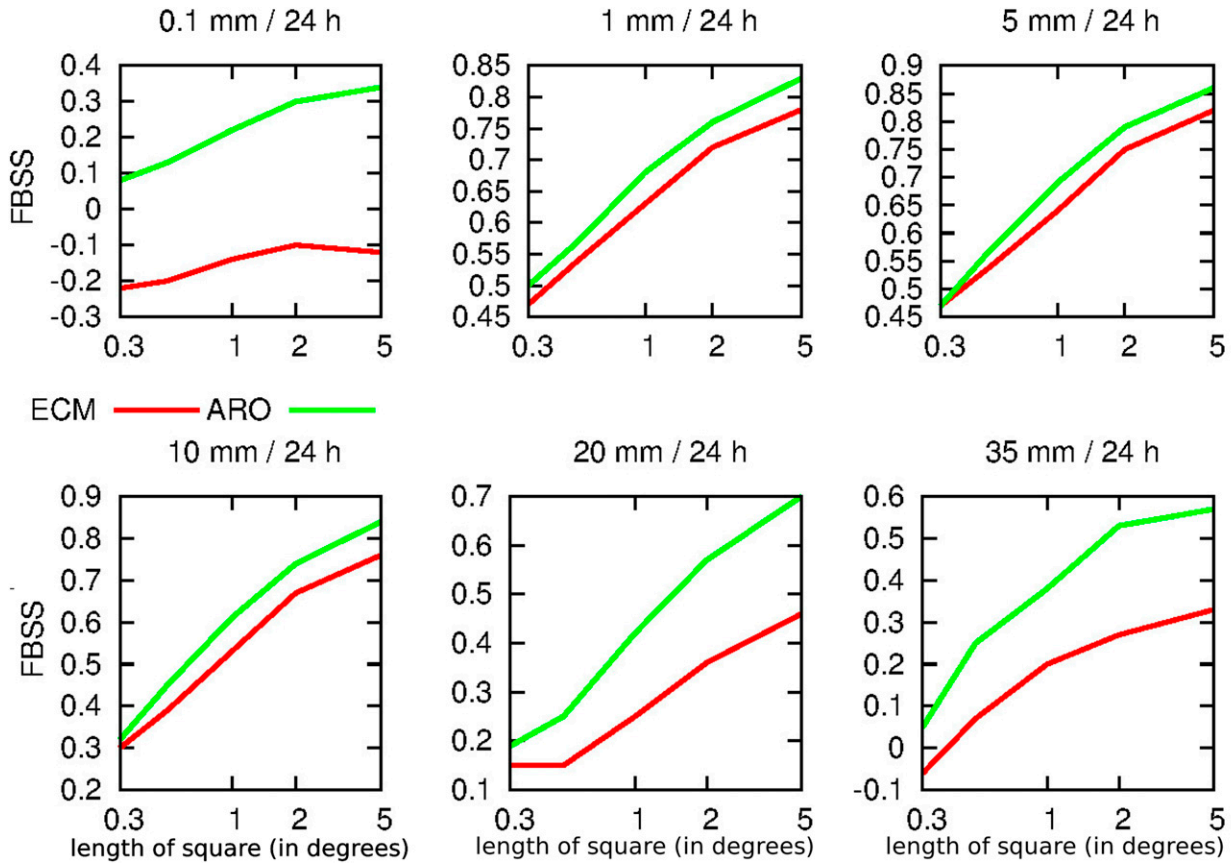


FIG. 11. FBSS analysis for 24-h accumulated precipitation. The square size is given along the *x* axis and FBSS along the *y* axis. Scores are shown for various precipitation thresholds [0.1, 1, 5, 10, 20, and 35 mm (24 h)$^{-1}$] for the ECMWF-IFS (red lines) and AROME-MetCoOP (green lines) systems. The validation period is from October 2014 to June 2015.

precipitation rates were not extreme; however, the continuous strong rainfall over several days caused severe flooding and landslides. The weather situation originally arose from the strong Tropical Cyclone Gonzalo in the Caribbean Sea, which developed 12 October and intensified for several days into a major hurricane (category 4), being the strongest since 2011. The remaining extratropical storm followed a storm track toward the coastline of western Norway. This low pressure system with warm and humid air formed the basis for the strong precipitation during 26–28 October, with peak values on 28 October.

In general, the weather pattern and timing of the most extreme precipitation period was well predicted by the ECMWF-IFS large-scale model. However, for a prediction of floods and landslides the localization and the amount of precipitation are crucial. We compare 48-hourly accumulated precipitation obtained from the rain gauge network and forecasts of the ECMWF-IFS and AROME-MetCoOp models (Fig. 13). The higher-resolution AROME-MetCoOp model shows an improved representation of the localized rainfall location and intensity. In the coarser-resolution ECMWF-IFS model the locations with high precipitation rates (i.e., larger than 50 mm) are generally underestimated. Instead, the AROME-MetCoOp model captures the amount and location of large precipitation events reasonably well. Validation of an individual time series shows the well-defined timing of the most extreme precipitation by both models, and further, the ability of AROME-MetCoOp to capture the large precipitation amounts realistically (Fig. 14). The main reason for a more realistic forecast of AROME-MetCoOp compared with the large-scale ECMWF-IFS model is the improved representation of orographic forcing (see also Figs. 1b,c).

### c. *Storm along the Norwegian west coast*

In the beginning of February 2015 a deep low pressure system developed in the Norwegian Sea accompanied by strong winds as the primary threat. The potential of an extreme wind event was well forecasted

www.manaraa.com

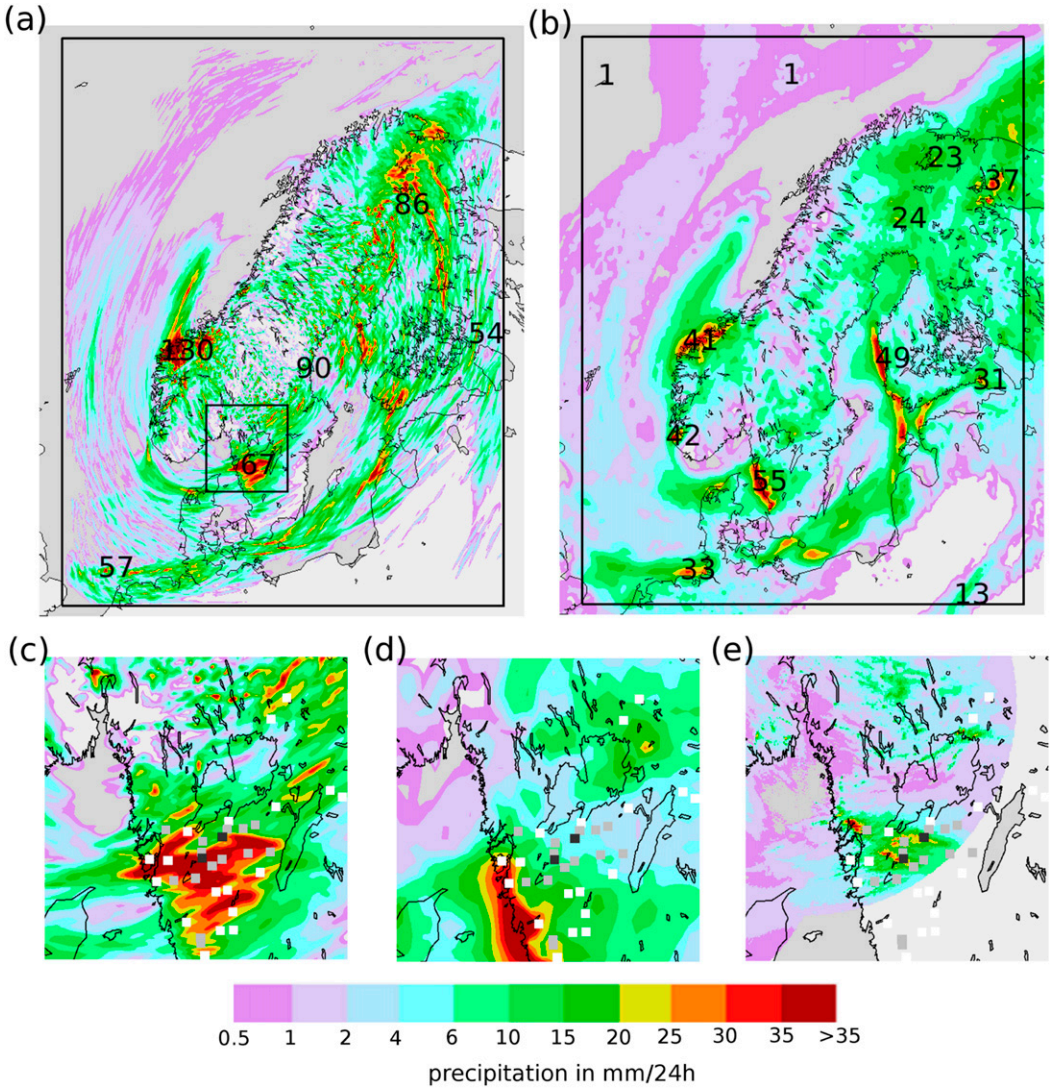


FIG. 12. The 24-h accumulated precipitation (mm) at 0600 UTC 20 Aug 2014 from (a) AROME-MetCoOp and (b) ECMWF-IFS forecasts initialized at 0000 UTC 19 Aug 2014. Black numbers indicate the maxima of the simulated precipitation. (c),(d) As in (a),(b), but for a small area in the southern part of the domain (southern Sweden). (e) The radar precipitation product from the Norwegian radar located at Hurum. The squares in (c), (d), and (e) highlight the measurements from the Swedish rain gauge network and are color coded as follows: white, 20–40; gray, 40–100; and black, $\geq$100 mm $(24\,\text{h})^{-1}$.

by ECMWF-IFS with quite consistent forecasts of where landfall of the low pressure system would take place.

In the morning of 7 February the storm center hit the northern Norwegian coast (Fig. 15), and the pressure field generated a strong northwesterly flow perpendicular to the Norwegian coast. This wind direction in combination with strong wind conditions leads to strong winds and gusts in the Norwegian fjords and farther inland. Even though warnings were issued early, major damage to infrastructure was reported.

Both the ECMWF-IFS and AROME-MetCoOp forecasts showed good agreement with the model analysis for MSLP, indicating a well-forecasted low pressure system on the synoptic scale. However, with increasing lead times of the forecasts there are differences in the exact locations of the strongest winds and in the magnitude of the wind speeds (not shown). The most striking difference between AROME-MetCoOp and ECMWF-IFS is in the higher wind speeds in AROME-MetCoOp. It is a known deficiency of AROME-MetCoOp that winds are too high in extreme situations. However, for this case data were available to confirm such behavior. Over land areas scatterplots show a significantly better level of performance for AROME-MetCoOp than ECMWF-IFS

المنارة للاستشارات
www.manaraa.com

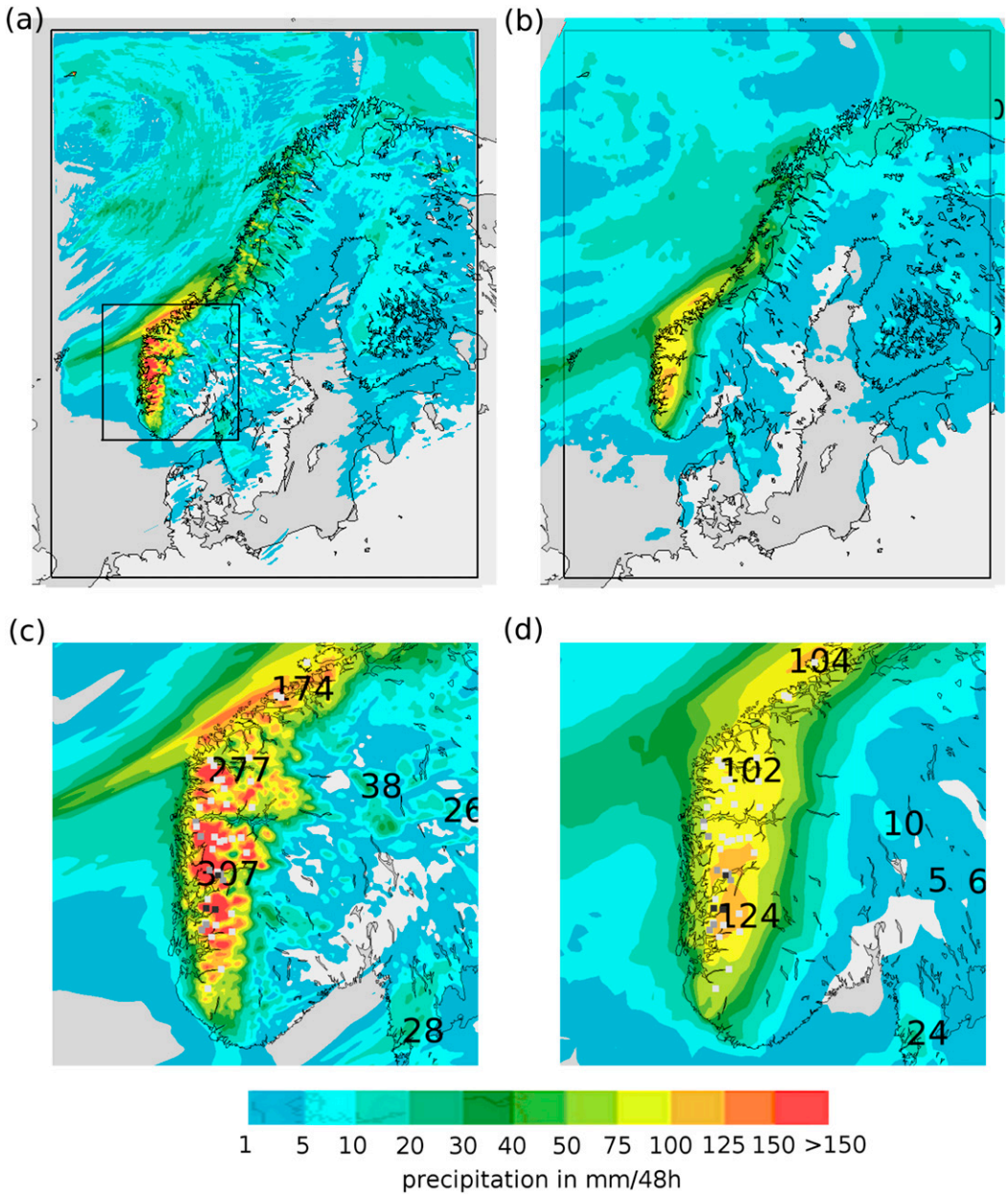


FIG. 13. The 48-h accumulated precipitation (mm) at 0600 UTC 30 Oct 2014 from (a) AROME-MetCoOp and (b) ECMWF-IFS forecasts initialized at 0000 UTC 28 Oct 2014. Black numbers indicate the maxima of the simulated precipitation. (c),(d) As in (a),(b), but for a smaller area over southern Norway. The squares in (c) and (d) highlight the measurements from the Norwegian rain gauge network and are color coded as follows: white, 100–150; gray, 150–200; and black, ≥200 mm $(48\,\mathrm{h})^{-1}$.

(Fig. 16). While AROME-MetCoOp scatters along the diagonal, the ECMWF-IFS wind forecasts are underestimated at almost all observation points. On average, in ECMWF-IFS the wind magnitude is underestimated and, generally, the system is not able to capture high wind speeds. AROME-MetCoOp shows much better agreement and is able to forecast high wind speeds. However, there is significant scatter for both models, which indicates that the forecast skill with respect to local details has deficiencies.

## 6. Summary and outlook

In the present paper we describe the operational usage of a high-resolution, nonhydrostatic, convective-scale weather prediction model for the Nordic regions.

www.manaraa.com

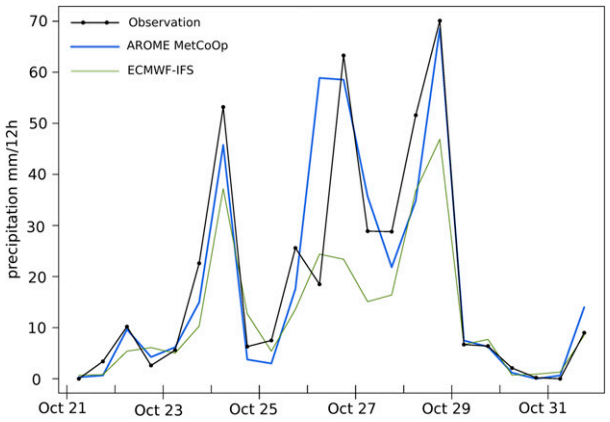


FIG. 14. Time series of 12-h accumulated precipitation observations and forecasts [mm $(12\,h)^{-1}$] at Kvamskogen, Norway. The observation site is in the Norwegian mountains and is visible in Fig. 13c, in the center of the number 307, which displays the local maximum of forecasted precipitation. The observations are at 0600 and 1800 UTC (black). The 18-h forecasts from AROME-MetCoOp (blue) and ECMWF-IFS (green) initialized at 0000 and 1200 UTC are used.

The convective-scale AROME-MetCoOp model has been in operation since March 2014 and is tuned and adapted to the specifications of our Nordic model domain. Modifications are made to the surface boundary layer parameterization as a result of the introduction of the new physiography ECOCLIMAP2 product. Furthermore, the microphysics needed modifications because of the sparsity of supercooled liquid water clouds in the case of moderate cold weather and too many low-level ice clouds in the case of very cold weather.

Several observation types are assimilated in the surface and upper-air atmospheric model. In the atmosphere we use a spectral mixing scheme, which mixes large-scale information of the ECMWF-IFS with the AROME-MetCoOp model's background. The spectral nudging is followed by a 3DVAR data assimilation scheme using climatological model error covariances. Conventional observations, such as data from SYNOP stations, drifting buoys, radiosondes, and airplanes together with ATOVS satellite observations are included in the 3DVAR minimization. In addition, two new high-resolution observations, radar reflectivity from the Norwegian and Swedish radar network and ground-based GNSS ZTD observations, are included.

The 1-yr model verification and comparison against the ECMWF-IFS highlights the strengths of the high-resolution model. ECMWF-IFS has issues in forecasting precipitation (RR12) values larger than 15 mm and wind speeds larger than $10\,m\,s^{-1}$, and it is found that AROME-MetCoOp clearly adds value to those forecast parameters. Also for temperature, the high resolution of the AROME-MetCoOp model considerably improves the forecasts in the complex topography of the Norwegian mountains, and the cold temperature bias of the ECMWF-IFS model is reduced by the AROME-MetCoOP model.

Since the operational use of AROME-MetCoOp began, several extreme events connected to strong winds or precipitation occurred. We chose three events for this study. The first event is a small-scale convective precipitation event in southern Sweden, where large amounts of precipitation led to local flooding and damage. The second case is a large-scale precipitation event in the Norwegian mountains, which resulted in heavy flooding in some canyons. And the third event represents a storm that occurred along the northern Norwegian coast with very strong winds as the main threat to local communities and industries. All three events were well forecasted by AROME-MetCoOp, and a timely information flow was initiated to warn local authorities and the public.

The two events along the Norwegian west coast (storm and large-scale precipitation) were embedded in a large-scale atmospheric flow system and, thus, were generally well forecasted by the ECMWF-IFS model. However, the improved representation of small-scale processes and surface parameters enabled AROME-MetCoOp forecasts to improve the magnitudes and locations of the maximum wind speed and precipitation. This information is of considerable importance when warnings are being issued by the meteorological services on severe weather situations and for further use in downstream impact models (e.g., hydrological models).

Because of the small-scale characteristics of the convective processes, the strong convective precipitation event in southern Sweden was not captured by the ECMWF-IFS model at all, but was reasonably well forecasted by AROME-MetCoOp. However, even though the AROME-MetCoOp resolves convective processes and produces consistent magnitudes of precipitation, the forecasting of the exact location is not possible. Presumably, the assimilation of more high-resolution observations will improve the model forecasts in this respect (Chang et al. 2014). Furthermore, the stochastic character and fast development of convective cells emphasizes the need to use an ensemble prediction system rather than deterministic forecasts (Schwartz et al. 2015). Indeed, the latter is envisaged for the year 2016, when a suite of 10 AROME-MetCoOp ensemble members will be in operation.

In the near future it is planned to include more observations in the data assimilation system, such as satellite observations from the Infrared Atmospheric Sounding Interferometer (IASI), the Advanced

www.manaraa.com

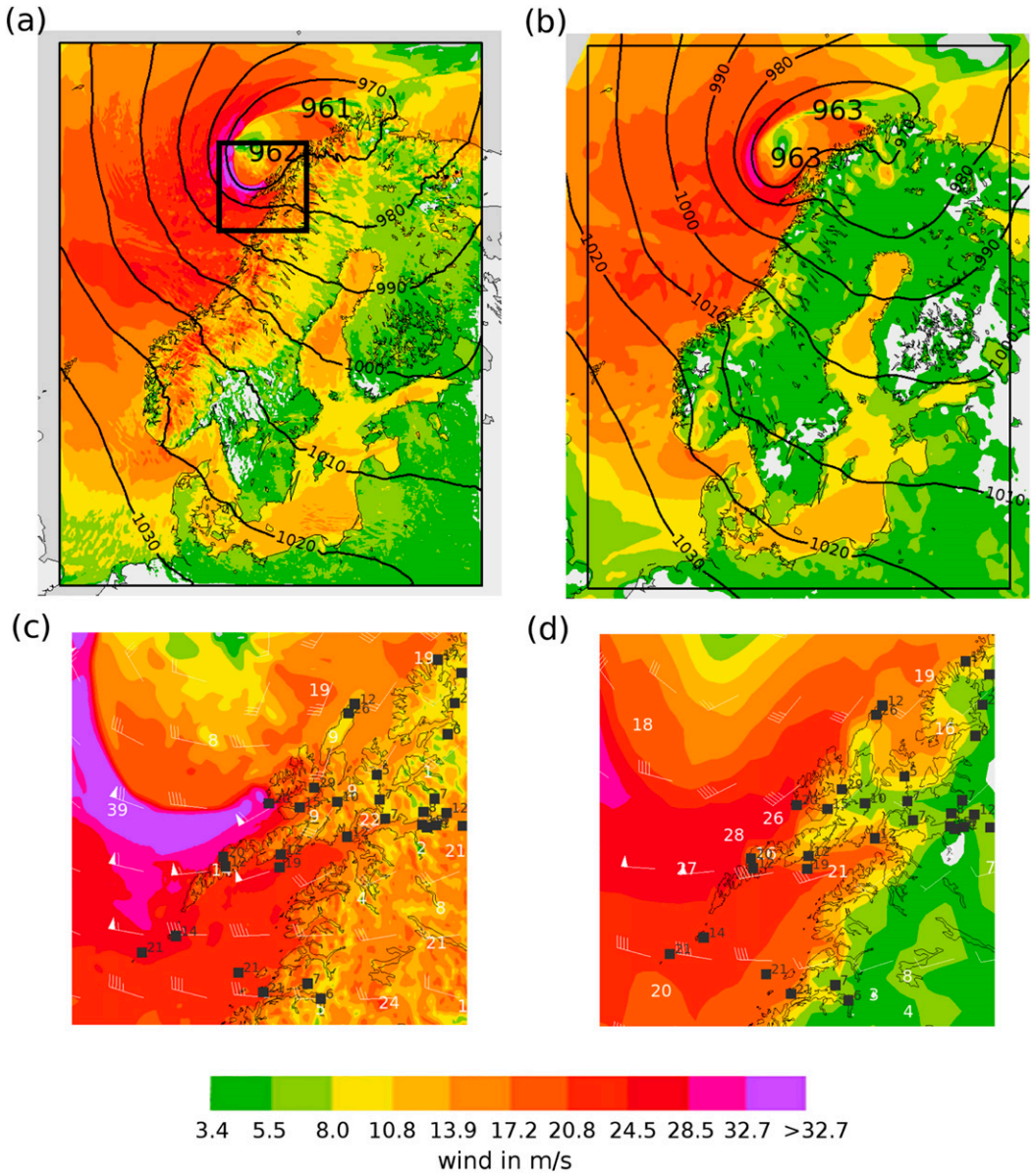


FIG. 15. Color-contoured wind speed ($m\,s^{-1}$) and black contour lines for MSLP (hPa) at 0800 UTC 7 Feb 2015 from (a) AROME-MetCoOp and (b) ECMWF-IFS forecasts initialized at 0000 UTC 7 Feb 2015. Black numbers indicate MSLP. (c),(d) As in (a),(b), but for a smaller area over western Norway. White numbers indicate maximum wind speeds. Black dots and numbers indicate observed wind speeds.

Scatterometer (ASCAT; Valkonen et al. 2016), and atmospheric motion vectors (AMVs), radar Doppler winds, radar data from the radar networks of Denmark and Finland, and a considerably increased amount (about 600) of GNSS ZTD observations. Also, the use of sea surface temperature (SST) from high-resolution ocean models is progressing, and it is expected that soon, for the Baltic Sea, the SST will be prescribed by an operational ocean model. Sensitivity experiments show that this has a positive impact, specifically for weather forecasts along the coast. Concerning forecasting issues in higher-latitude regions, developments in the parameterization of shallow convection are ongoing and a more advanced three-layer snow scheme is currently being tested.

The forecasting system is currently operated as a cooperative venture between the Norwegian and Swedish weather services (MetCoOp). This cooperation between two national weather services is unique and will be further expanded in the future with the NORDNWP

www.manaraa.com

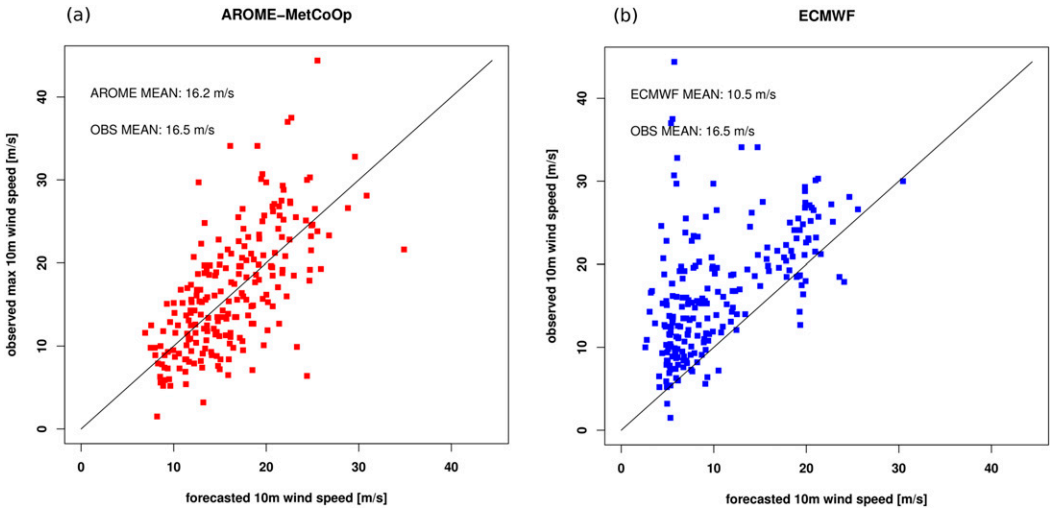


FIG. 16. Scatterplots of the mean of the maximum 10-min wind speeds ($m\,s^{-1}$) for 8 Feb 2015 for observations obtained from (a) AROME-MetCoOp and (b) ECMWF-IFS for all Norwegian weather stations.

cooperation project, where the national meteorological services of the five Nordic countries, Denmark, Finland, Iceland, Norway, and Sweden, are aiming for the common production of numerical weather prediction. The NORDNWP project was initiated in 2015, and it is planned to operate a common model suite by the year 2020 on a joint high-performance computing infrastructure.

*Acknowledgments.* The ALADIN HIRLAM system was made available by the ALADIN and HIRLAM Consortia involving the national meteorological services of Norway and Sweden. MM acknowledges support from Norwegian Research Council Grants 216034 and 256399. We thank the editor and three two anonymous reviewers for valuable comments and discussions.

## APPENDIX

### Spectral Mixing of Large-Scale Information

As a first step in the data assimilation procedure, the large-scale information from the host model is mixed into the model background. The control variables of the host model $\mathbf{x}_h$ are mixed into the model background $\mathbf{x}_b$ by

$$\tilde{\mathbf{x}}_b(m,n,l) = w(m,n,l)\cdot\mathbf{x}_h(m,n,l) + [1-w(m,n,l)]\cdot\mathbf{x}_b(m,n,l). \quad \text{(A1)}$$

The weighting function $w(m, n, l)$ depends on the horizontal wavenumbers $(m, n)$ and vertical levels $l$ and represents a simple spectral mixing scheme, whose characteristics are, in general, equivalent to adding a third term ($J_k$ term) to the cost function (Dahlgren and Gustafsson 2012):

$$J(\mathbf{x}) = J_b(\mathbf{x}) + J_o(\mathbf{x}) + J_k(\mathbf{x}). \quad \text{(A2)}$$

The cost function is written in detail as

$$J(\mathbf{x}) = \frac{1}{2}(\mathbf{x}-\mathbf{x}_b)^{\mathrm{T}}\mathbf{B}^{-1}(\mathbf{x}-\mathbf{x}_b) + \frac{1}{2}(\mathbf{y}-\mathbf{H}\mathbf{x})^{\mathrm{T}}\mathbf{R}^{-1}(\mathbf{y}-\mathbf{H}\mathbf{x}) + \frac{1}{2}(\mathbf{x}-\mathbf{x}_h)^{\mathrm{T}}\mathbf{V}^{-1}(\mathbf{x}-\mathbf{x}_h), \quad \text{(A3)}$$

where the $\mathbf{R}$, $\mathbf{B}$, and $\mathbf{V}$ matrices represent the observation, model background error, and host-model background-error covariances. The optimal solution of $\mathbf{x}$ is found where $\nabla J = 0$. We assume that $\tilde{\mathbf{x}}_b$ is a combination of the model background $\mathbf{x}_b$ and the host model $\mathbf{x}_h$ and write the cost function in the form

$$J(\mathbf{x}) = \frac{1}{2}(\mathbf{x}-\tilde{\mathbf{x}}_b)^{\mathrm{T}}\tilde{\mathbf{B}}^{-1}(\tilde{\mathbf{x}}-\tilde{\mathbf{x}}_b) + \frac{1}{2}(\mathbf{y}-\mathbf{H}\mathbf{x})^{\mathrm{T}}\mathbf{R}^{-1}(\mathbf{y}-\mathbf{H}\mathbf{x}). \quad \text{(A4)}$$

It can then be shown that

$$\tilde{\mathbf{x}}_b = \mathbf{V}(\mathbf{B}+\mathbf{V})^{-1}\mathbf{x}_b + \mathbf{B}(\mathbf{B}+\mathbf{V})^{-1}\mathbf{x}_h \quad \text{and} \quad \text{(A5)}$$

$$\tilde{\mathbf{B}} = (\mathbf{B}^{-1}+\mathbf{V}^{-1})^{-1}. \quad \text{(A6)}$$

Thus, we can conclude that a 3DVAR minimization with the $J_k$ term is equivalent to a minimization without the $J_k$ term but with a premixing of the large-scale model information according to (A5), and using a modified covariance matrix [(A6)] for the premixing first-guess $\tilde{\mathbf{x}}_b$.

www.manaraa.com

## REFERENCES


Bauer, P., and Coauthors, 2013: Model cycle 38r2: Components and performance. ECMWF Tech. Memo. 704, 58 pp. [Available online at http://www.ecmwf.int/en/elibrary/7986-model-cycle-38r2-components-and-performance.]

Berre, L., 2000: Estimation of synoptic and mesoscale forecast error covariances in a limited-area model. *Mon. Wea. Rev.*, **128**, 644–667, doi:10.1175/1520-0493(2000)128<0644:EOSAMF>2.0.CO;2.

Brossier, C. L., V. Ducrocq, and H. Giordani, 2009: Two-way one-dimensional high-resolution air–sea coupled modelling applied to Mediterranean heavy rain events. *Quart. J. Roy. Meteor. Soc.*, **135**, 187–204, doi:10.1002/qj.338.

Brousseau, P., L. Berre, F. Bouttier, and G. Desroziers, 2012: Flow-dependent background-error covariances for a convective-scale data assimilation system. *Quart. J. Roy. Meteor. Soc.*, **138**, 310–322, doi:10.1002/qj.920.

Caumont, O., V. Ducrocq, E. Wattrelot, G. Jaubert, and S. Pradier-Vabre, 2010: 1D+3DVar assimilation of radar reflectivity data: A proof of concept. *Tellus*, **62**, 173–187, doi:10.1111/j.1600-0870.2009.00430.x.

Chang, W., K.-S. Chung, L. Fillion, and S.-J. Baek, 2014: Radar data assimilation in the Canadian high-resolution ensemble Kalman filter system: Performance and verification with real summer cases. *Mon. Wea. Rev.*, **142**, 2118–2138, doi:10.1175/MWR-D-13-00291.1.

Dahlgren, P., 2013: A comparison of two large scale blending methods: $J_k$ and LSMIXBC. METCOOP Memo. 2, Norwegian Meteorological Institute and Swedish Meteorological and Hydrological Institute, 10 pp. [Available online at http://metcoop.org/memo/2013/02-2013-METCOOP-MEMO.PDF.]

——, and N. Gustafsson, 2012: Assimilating host model information into a limited area model. *Tellus*, **64**, 15836, doi:10.3402/tellusa.v64i0.15836.

Davies, H. C., 1976: A lateral boundary formulation for multi-level prediction models. *Quart. J. Roy. Meteor. Soc.*, **102**, 405–418, doi:10.1002/qj.49710243210.

Dee, D., 2005: Bias and data assimilation. *Quart. J. Roy. Meteor. Soc.*, **131**, 3323–3334, doi:10.1256/qj.05.137.

Donier, S. Y., S. Faroux, and V. Masson, 2012: Evaluation of the impact of the use of the ECOCLIMAP2 database on AROME operational forecasts. Météo-France Tech. Rep., 89 pp. [Available online at http://www.umr-cnrm.fr/surfex/IMG/pdf/test_eco2_arome.pdf.]

Donlon, C. J., M. Martin, J. Stark, J. Roberts-Jones, E. Fiedler, and W. Wimmer, 2012: The Operational Sea Surface Temperature and Sea Ice Analysis (OSTIA) system. *Remote Sens. Environ.*, **116**, 140–158, doi:10.1016/j.rse.2010.10.017.

Ebert, E. E., 2008: Fuzzy verification of high-resolution gridded forecasts: A review and proposed framework. *Meteor. Appl.*, **15**, 51–64, doi:10.1002/met.25.

Faroux, S., A. T. Kaptué Tchuenté, J.-L. Roujean, V. Masson, E. Martin, and P. Le Moigne, 2013: ECOCLIMAP-II/Europe: A twofold database of ecosystems and surface parameters at 1 km resolution based on satellite information for use in land surface, meteorological and climate models. *Geosci. Model Dev.*, **6**, 563–582, doi:10.5194/gmd-6-563-2013.

Guidard, V., and C. Fischer, 2008: Introducing the coupling information in a limited-area variational assimilation. *Quart. J. Roy. Meteor. Soc.*, **134**, 723–735, doi:10.1002/qj.215.

Homleid, M., and M. A. Killie, 2013: HARMONIE snow analysis experiments with additional observations. Norwegian Meteorological Institute Tech. Rep. 6, 21 pp. [Available online at https://met.no/filestore/snow_report.pdf.]

Kristiansen, J., S. L. Sørland, T. Iversen, D. Bjørge, and M. O. Køltzow, 2011: High-resolution ensemble prediction of a polar low development. *Tellus*, **63A**, 585–604, doi:10.1111/j.1600-0870.2010.00498.x.

Masson, V., J.-L. Champeaux, F. Chauvin, C. Meriguet, and R. Lacaze, 2003: A global database of land surface parameters at 1-km resolution in meteorological and climate models. *J. Climate*, **16**, 1261–1282, doi:10.1175/1520-0442-16.9.1261.

——, and Coauthors, 2013: The SURFEXv7.2 land and ocean surface platform for coupled or offline simulation of earth surface variables and fluxes. *Geosci. Model Dev.*, **6**, 929–960, doi:10.5194/gmd-6-929-2013.

Montmerle, T., and L. Berre, 2010: Diagnosis and formulation of heterogeneous background-error covariances at the mesoscale. *Quart. J. Roy. Meteor. Soc.*, **136**, 1408–1420, doi:10.1002/qj.655.

Pinty, J.-P., and P. Jabouille, 1998: A mixed-phased cloud parameterization for use in a mesoscale non-hydrostatic model: Simulations of a squall line and of orographic precipitation. Preprints, *Conf. on Cloud Physics*, Everett, WA, Amer. Meteor. Soc., 217–220.

Randriamampianina, R., 2006: Impact of high resolution observations in the ALADIN/HU model. *Idojaras*, **110**, 329–349.

——, T. Iversen, and A. Storto, 2011: Exploring the assimilation of IASI radiances in forecasting polar lows. *Quart. J. Roy. Meteor. Soc.*, **137**, 1700–1715, doi:10.1002/qj.838.

Roberts, N. M., and H. W. Lean, 2008: Scale-selective verification of rainfall accumulations from high-resolution forecasts of convective events. *Mon. Wea. Rev.*, **136**, 78–97, doi:10.1175/2007MWR2123.1.

Sánchez Arriola, J., M. Lindskog, S. Thorsteinsson, and J. Bojarova, 2016: Variational bias correction of GNSS ZTD in the HARMONIE modeling system. *J. Appl. Meteor. Climatol.*, **55**, 1259–1276, doi:10.1175/JAMC-D-15-0137.1.

Schwartz, C. S., G. S. Romine, M. L. Weisman, R. A. Sobash, K. R. Fossell, K. W. Manning, and S. B. Trier, 2015: A real-time convection-allowing ensemble prediction system initialized by mesoscale ensemble Kalman filter analyses. *Wea. Forecasting*, **30**, 1158–1181, doi:10.1175/WAF-D-15-0013.1.

Seity, Y., P. Brousseau, S. Malardel, G. Hello, P. Bénard, F. Bouttier, C. Lac, and V. Masson, 2011: The AROME-France convective-scale operational model. *Mon. Wea. Rev.*, **139**, 976–991, doi:10.1175/2010MWR3425.1.

Simmons, A. J., and D. M. Burridge, 1981: An energy and angular-momentum conserving vertical finite-difference scheme and hybrid vertical coordinates. *Mon. Wea. Rev.*, doi:**109**, 758–766, 10.1175/1520-0493(1981)109<0758:AEAAMC>2.0.CO;2.

Sun, J., 2005: Convective-scale assimilation of radar data: progress and challenges. *Quart. J. Roy. Meteor. Soc.*, **131**, 3439–3463, doi:10.1256/qj.05.149.

Taillefer, F., 2002: CANARI: Technical documentation. CNRM/GMAP Internal Rep., Météo-France, 55 pp. [Available online at http://www.cnrm.meteo.fr/gmapdoc/spip.php?article3.]

Valkonen, T., H. Schyberg, and J. Figa-Saldana, 2016: Assimilating Advanced Scatterometer winds in a high-resolution limited area model over northern Europe. *IEEE J. Sel. Top. Appl. Earth Obs. Remote Sens.*, **PP** (99), 1–12, doi:10.1109/JSTARS.2016.2602889.

Von Storch, H., H. Langenberg, and F. Feser, 2000: A spectral nudging technique for dynamical downscaling purposes. *Mon. Wea. Rev.*, **128**, 3664–3673, doi:10.1175/1520-0493(2000)128<3664:ASNTFD>2.0.CO;2.

Wattrelot, E., O. Caumont, and J.-F. Mahfouf, 2014: Operational implementation of the 1D+3D-Var assimilation method of radar reflectivity data in the AROME model. *Mon. Wea. Rev.*, **142**, 1852–1873, doi:10.1175/MWR-D-13-00230.1.


www.manaraa.com

Reproduced with permission of copyright owner. Further reproduction prohibited without permission.

www.manaraa.com